Optimization of Orifices Arrangement for the Maximized Spray Tip Penetration of Wall-Impinging Sprays Injected by Group-Hole Nozzles

S. Moon*, Y. Matsumoto and K. Nishida
Department of Mechanical System Engineering, University of Hiroshima
1-4-1, Kagamiyama, Higashi-Hiroshima, 739-8527, Japan

J. Gao
Department of Mechanical Engineering, University of Wisconsin-Madison
1500 Engineering Drive, Madison, WI 53706, USA
Rolla, MO 65409-0050 USA

Abstract

In this study, the factors related to the optimization of wall-impinging sprays injected by closely spaced micro-orifices (group hole nozzle) were investigated to improve the in-cylinder air utilization by enhancing the spray tip penetration after wall-impingement. To maximize the spray tip penetration of group hole nozzle sprays, the different types of group hole nozzles, which have different intervals and angles between orifices, were applied in this study. The spray tip penetration of evaporating sprays were measured based on the optical thickness images captured using a laser absorption scattering (LAS) technique.

The results showed that the distance between the arbitrary centers of two impinging jets at the impingement wall (χ) has the significant effect on the spray tip penetration of group hole nozzles. The elliptical shape of spray was observed for all test nozzles although the ratio between major axis and minor axis of ellipse was different for each nozzle. The elliptical shape of wall-impinging spray was changed with time and the crossing timing when the minor axis starts to be major axis appeared earlier as the χ distance decreased and the injection pressure increased. The spray tip penetration of group hole nozzle spray was maximized around the χ distance of 5.4mm where the strong momentum region of each jet starts to interact just after the wall-impingement. The related mechanism on this phenomenon was discussed in terms of (1) the momentum separation of each jet to the penetrating direction and the spray axis direction and (2) the momentum interaction of two jets after wall-impingement.

Introduction

Recent diesel fuel injection system prefers the smaller orifice diameter with larger number of holes to improve fuel evaporation and consequently air utilization inside the combustion chamber [1, 2]. Lots of researches have been investigated the effect of orifice diameter on mixture formation process and flame structure [1-3]. The improved mixing of fuel and air and longer flam lift-off length were observed at smaller orifice diameters. Also, previous researches on engine combustion revealed that the high injection pressure with micro-orifices can be effective in low and partial loads conditions [2, 4-7]. Nevertheless, the shorter spray tip penetration of these nozzles can be a drawback in high speed and load conditions. The weakened interaction between fuel spray and piston cavity, caused by the shorter spray tip penetration, decreases the air utilization inside the piston cavity and finally increases the soot emission at high load and speed conditions [7, 8].

The concept of group hole nozzle that equips the closely located two micro-orifices has been introduced to improve the evaporation characteristics of spray without the sacrifice in the spray tip penetration to overcome the disadvantage of micro-orifices [9-11]. Figure 1 shows the conceptual diagram of group hole nozzle compared to the single hole nozzle. From the previous results, it was found that the group hole nozzle spray has some advantage in fuel evaporation without the sacrifice in spray tip penetration in free spray condition [9]. However, outstanding advantage from group hole nozzle spray arises from the wall-impinging sprays. From the previous researches, it was found that the shape of group hole nozzle spray after wall-impingement is asymmetrical, thus spray tip penetration increased to a certain direction (upside and downside in Fig. 2) and decreased to another direction [10, 11]. From the deposit image of spray (left image in Fig. 2), outward bulges were found and it confirmed above explanation. At the moment of wall-impingement, the momentum interaction of two close jets results in a strong flow along a line,

*Corresponding author, hiromoon@hiroshima-u.ac.jp

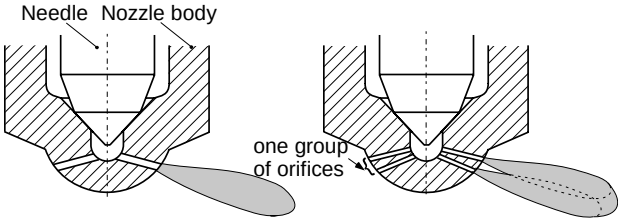

Fig. 1 Conceptual diagram of single hole nozzle and group hole nozzle [(a) Single hole nozzle concept, (b) Group hole nozzle concept]

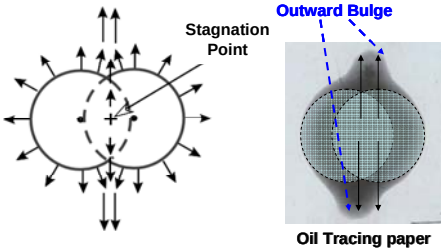

Fig. 2 A theoretical diagram of fuel flow after impingement [13] (left) and the deposit generated from group hole nozzle spray (right)

which vertically crosses a center point of a line connecting the centers of two circles [10, 11], as shown in the right image of Fig. 2. Correspondingly, if the nozzle alignment is optimized to make the longer penetration region head to the central region of the piston cavity, the air utilization inside the combustion chamber could be enhanced and consequently the soot emission will be reduced.

Although there have been comparative researches about the spray development of group hole nozzle and conventional single hole nozzle, the detailed strategy for the maximization of spray tip penetration was not yet discussed. The aim of this research is to find out the factors which determine the wall-impinging spray tip penetration of group-hole nozzles to obtain the maximized spray tip penetration. To find out the optimization factors and related mechanism, various types of group-hole nozzles were designed and applied with the variance in the angles and distances between micro-orifices. The geometry of wall-impinging spray was analyzed using a LAS technique. Based on the experimental results, a conceptual diagram explaining the mechanism related to the wall-impinging spray tip penetration was introduced.

Experimental Setup and Conditions

Setup for Spray Imaging at Evaporating Condition

The principle of LAS, requirement on the test fuel and the possible measurement error were discussed in the previous researches [12, 13]. In this study, the results of spray geometry for evaporating sprays obtained by the LAS technique were only considered for discussion. The LAS measurements were implemented in a high temperature and high pressure constant volume vessel. A schematic diagram of the optical arrangement of the LAS imaging system, the fuel injection system and the constant volume vessel is shown in Fig. 3. A pulsed Nd:YAG laser (NY61-10, Continuum) was employed to provide the two wavelength beams, one at ultraviolet (UV) 266nm (absorption wavelength) and the other at visible (Vis) 532nm (transparent wavelength). The two beams were separated by a dichroic mirror, and were magnified into a diameter of 100mm by the beam expanders. In order to minimize the schlieren-like effect due to the ambient gas density gradient on the LAS image, a diffuser was set between the first harmonic mirror and the window of the vessel. After transmitted to the spray, the two beams were focused again and captured by two CCD cameras (Photonics C4880, Hamamatsu, 384×576 pixels and 12bit grayscale). The images acquisition and arithmetic processing were carried out by an IPLab (Spectrum Signal Analytics) image analysis system. The laser pulse was triggered through the Q-switch of the Nd:YAG laser. A pulse generator (DG 535, Stanford Inc.) was used to synchronize the Nd:YAG laser, the CCD cameras and the injection system.

Definitions on the Orifice Arrangement

Figure 4 shows the definitions on the orifice arrangement. The B distance was defined as the closest distance between the surfaces of each orifice when viewed by sac area. The included angles of α and β were defined as the angle between the orifices when viewed by y-axis. In case of α angle nozzle, the orifices were arranged along x-axis while these were arranged along y-axis in case of β nozzle. If the arbitrary centerlines of each jet are assumed, the distance between arbitrary centers of each jet (χ) can be calculated at the impingement wall. Two view directions were defined to explain the non-axisymmetric shape of group-hole nozzle sprays. If the included angle can be shown at a direction, this direction was defined as 'Vertical view direction' (viewed by y-axis) and the other direction was defined as 'Parallel view direction' (viewed by x-axis). The longer penetration after wall-impingement is observable from the Parallel view direction based on the previous researches [10, 11].

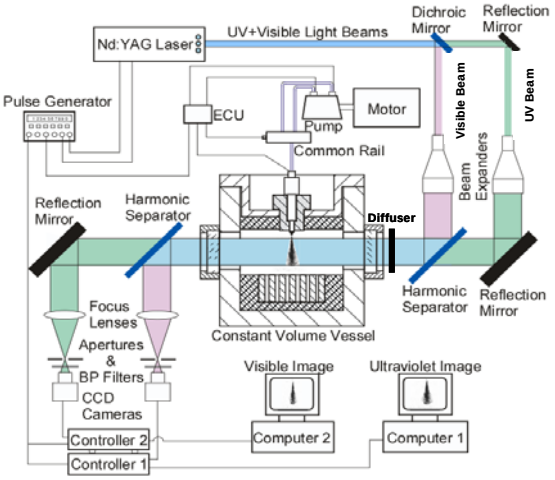

Fig. 3 Setup for Spray Imaging

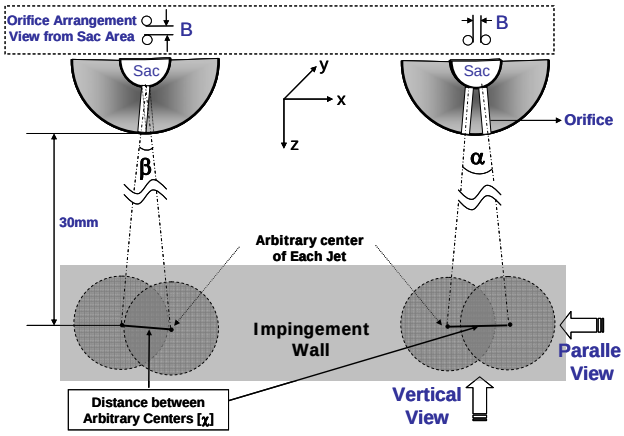

Fig. 4 Definitions on the orifice arrangement

Nozzle Specifications

Table 1 shows the specifications of the test nozzles. In Cases 1 and 2, different α and β angles were applied respectively and the range of angles was from 5° to 15°. The applied included angle was limited to 15° since the spray will be totally separated and the spray characteristics will be similar with micro-orifices if the included angle exceeds 15°. In Case 3, different B distances with an α angle of 10° were applied. The 10° α angle was selected as an optimized included angle and the details on it will be explained in the following sections. For all cases, the orifice diameter was 0.096mm. The corresponding χ distances for each orifice arrangement were also presented in Table 1.

Table 1 Specifications of Test Nozzles

Case 1					Case 2					Case 3				
Nozzle	B [mm]	α [deg]	β [deg]	χ [mm]	Nozzle	B [mm]	α [deg]	β [deg]	χ [mm]	Nozzle	B [mm]	α [deg]	β [deg]	χ [mm]
GHα5	0.194	5	–	2.91	GHβ5	0.204	–	5	2.64	GH/B0.098	0.098	10	–	5.44
GHα10	↑	10	–	5.54	GHβ10	↑	–	10	5.26	GH/B0.194	0.194	10	–	5.54
GHα15	↑	15	–	8.19	GHβ15	↑	–	15	7.90	GH/B0.290	0.290	10	–	5.63

Table 2 Experimental Conditions

	Abbreviation	Case 1	Case 2	Case 3
Injection Pressure	P_{inj} [MPa]	90	120	90
Injection Quantity	Q_{inj} [mg]	3.4	3.4	3.4
Ambient Pressure	P_{amb} [MPa]	4.0	4.0	4.0
Ambient Temp.	T_{amb} [K]	760	760	760
Fuel		1,3-dimethylnaphthalene [$C_{10}H_6(CH_3)_2$]		
Ambient Gas		Nitrogen (N_2)		
Impingement Distance		30mm		

Experimental Conditions

Table 2 shows the experimental conditions. For all cases, injection conditions and surrounding conditions were same except the injection pressure. Considering that the case 1 and Case 2 are similar orifices arrangement (included angle effect) and only the χ is slightly different, higher injection pressure (120MPa) was applied to Case 2 to investigate how the injection pressure affects on the group-hole nozzle spray development. DMN (1,3-dimethylnaphthalene) was selected as a test fuel based on the test fuel requirements for the LAS technique [12, 13]. To simulate the surrounding conditions of real engine, the ambient pressure and temperature were set to 4MPa and 760K respectively. To prevent possible combustion and for safety, nitrogen gas (N_2) which has similar molecular weight with air was used for the surrounding gas. The impingement distance was set to 30mm for each test case.

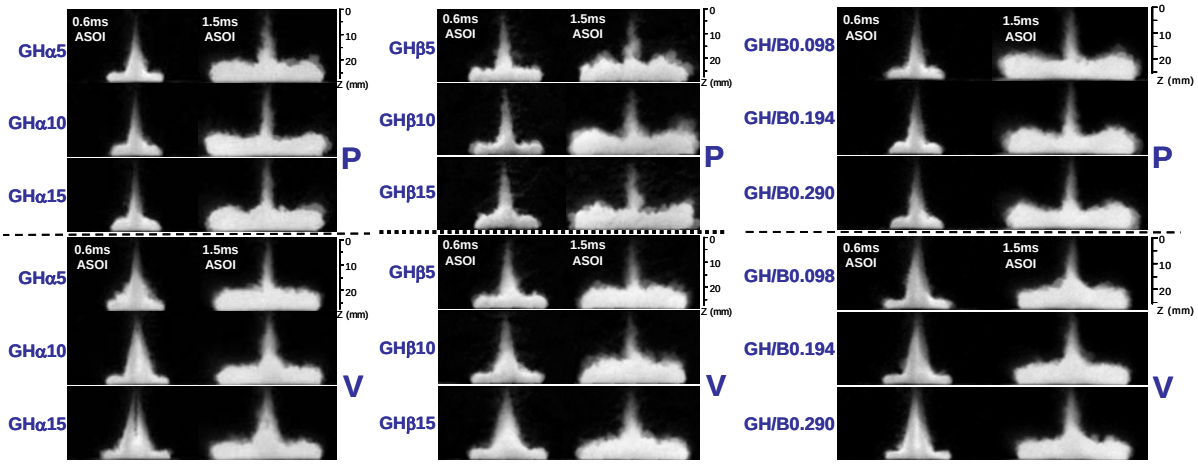

(a) Case 1 (b) Case2 (c) Case3

Fig. 5 Spray geometry of each test case at two view directions [The figures shown are optical thickness images. 'P' designates parallel view direction and 'V' designates parallel view direction.]

Results and Discussion

Spray Geometry

Figure 5 shows the optical thickness images of each test case. Optical thickness of vapor is a logarithm value of intensity attenuation when the spray is exposed to the absorption wavelength [12]. Just after the wall impingement, the penetration in vertical view direction was longer than that in parallel view direction and then the penetration in parallel view direction starts to overtake the penetration in vertical view direction. This higher rate of increase in penetration at parallel view direction is due to the momentum interaction between two jets after wall-impingement. However, the crossing time when the penetration of parallel view direction starts to be longer than that in vertical view direction and the increasing rate in spray tip penetration of parallel view direction appears differently for each nozzle. To explain this, the quantified spray tip penetration results at each case were presented in the next section.

Spray Tip Penetration

The spray tip penetration was defined as the summation of impingement distance and the half of radial spray length. Figure 6(a) shows the quantified spray tip penetration at each test case. At larger included angles, the spray tip penetration just after the wall-impingement in vertical view direction was longer than that at the smaller included angles as shown in Figs. 5(a) and 5(b). Two mechanisms are related to this phenomenon. One is the location of impingement point. If the included angle increases the spray impinges to the farther location from the spray axis and this will be a plus factor for the spray tip penetration in vertical view direction. Another reason is the difference in momentum separation to the spray axis direction and penetrating direction after wall impingement. At high included angle, the momentum of each jet heading to the penetrating direction is stronger than that to the spray axis and this causes longer penetration in vertical view direction at larger included angles.

In Cases 1 and 2, the included angle of 10^o and 15^o showed bigger increasing rate of spray tip penetration in parallel view direction than that in the included angle of 5^o. It means the strong momentum interaction of each jet after wall impingement appears for these nozzles. However, the crossing time appears later at high included angles since the longer χ distance cause later momentum interaction of each jet. The included angle of 10^o showed longest penetration in parallel view direction. It means the separated momentum to the spray axis direction and the momentum interaction of each jet are optimized at this included angle. The crossing time of spray tip penetration appeared earlier at higher injection pressure condition. The higher momentum of spray at higher injection pressure makes the impinging timing earlier and finally causes the momentum interaction to occur earlier. Above results support that the main mechanism related to the spray tip penetration of group hole nozzles is the momentum interaction of each jet after the wall-impingement.

Since it was found that the optimized momentum interaction occurs around the included angle of 10^o, the effect of B distance on the spray tip penetration at a fixed included angle of 10^o was investigated to find out the critical optimization point and then the results were presented in the third row of Fig. 6(a). The change in B distance causes the small change in χ distance as shown in Table 1. The results showed that the spray tip penetration increased and the crossing time appears earlier when the B distance decreased.

Figure 6(b) shows the spray tip penetration of each case at 1.5ms after the start of injection (ASOI) as a function of distance between arbitrary centers (χ). Based on this graph, there was an optimal χ for the maximization of spray tip penetration and the value was around 5.4mm. Around the optimization point (Region 1), severe change in the spray tip penetration was observed with the small variance in χ. If the χ is increased (Region 3) or decreased (Region 1) from the optimized value, the spray tip penetration starts to decrease. Although the spray tip penetration decreased for Cases 1 and 3 both, the related mechanism is quite different.

Discussion – Mechanism Related to the Spray Tip Penetration

The momentum interaction of each jet depends on the velocity distribution of each jet at the impinging instant. Generally, dense central region of spray has strong momentum and high velocity. Some previous researches suggested equations to describe the radial velocity distribution of the spray as shown in Eq. (1) [14].

$$U / U_0 = \exp(-2(r / R)^2) \quad (1)$$

where U is the axial velocity at a radial location, U_o is the axial velocity at the spray center, r is the radial location and R is the radial length of the spray. The exponential decrease of fuel velocity means there is a steep gradient in the fuel velocity along the radial location. This radial velocity distribution strongly affects the collision/coalescence of each jet. If strong momentum region of each jet interacts, severe collision/coalescence occurs and the larger droplets will be generated. The momentum of large droplets is stronger than that of smaller droplets and it leads to the longer spray tip penetration in the free spray condition [9]. However, in the wall-impinging condition, jet-to-jet interaction related to the spray tip penetration should be considered different way. The momentum interaction of each wall-impinging jet depends on the jet momentum at the impinging instant. If the jet-to-jet interaction occurs before wall-impingement, the initial momentum of each jet will be decreased at the impinging instant due to the momentum loss. Based on this concept, the mechanism related to the spray tip penetration will be explained for each region.

Region 1 (Strong Interaction of Two Wall Jets): In Region 1, the core regions of two jets, which have strong momentum, starts to meet each other just after the wall-impingement. Since these two core regions were separated before the wall impingement, the coalescence does not appear strongly and the two jets keep its initial momentum until the wall impingement. Just after the wall impingement, the spray-wall interaction of each jet starts to develop and it finally causes the strong momentum interaction between two wall-jets.

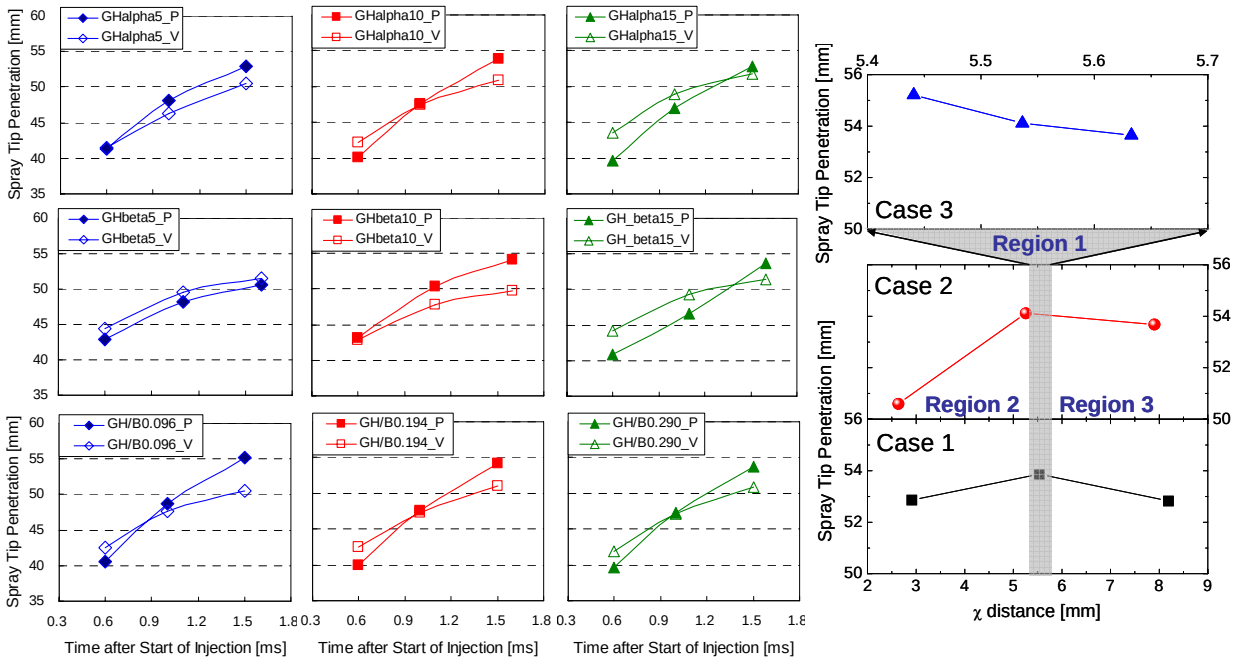

(a) (b)

Fig. 6 Quantified spray penetration results at different orifice arrangements (a) and spray tip penetration as a function of χ distance at 1.5ms ASOI (b)

Region 2 (Jet-to-Jet Interaction in the Near Field): In Region 2, dense and strong momentum region of two jets starts to meet in the near field. Due to the collision of dense core regions, the coalescence occurs severely and the spray characteristics is getting similar with the conventional single-orifice spray which has shorter spray tip penetration compared to the group hole nozzle spray [10, 11]. Another main reason for the reduced spray tip penetration at this region is the thicker liquid film thickness caused by the impingement of very dense coalesced region to the wall. This thicker liquid film attenuates the momentum of the spray and wall-jet interaction.

Region 3 (Weak Interaction of Two Wall-Jets): In Region 3, two jets impinge to the wall with relatively larger incident angle and longer χ distance compared to the optimized one. Due to this, the separated momentum heading to the spray axis is weaker than Region 1. Also, the strong momentum region of each spray has some distance at the wall-impinging instant, so it takes longer time the momentum of each spray to interact. During this delay, the spray loses its momentum to the wall-friction and finally the momentum interaction between two impinging jets will be much more weakened.

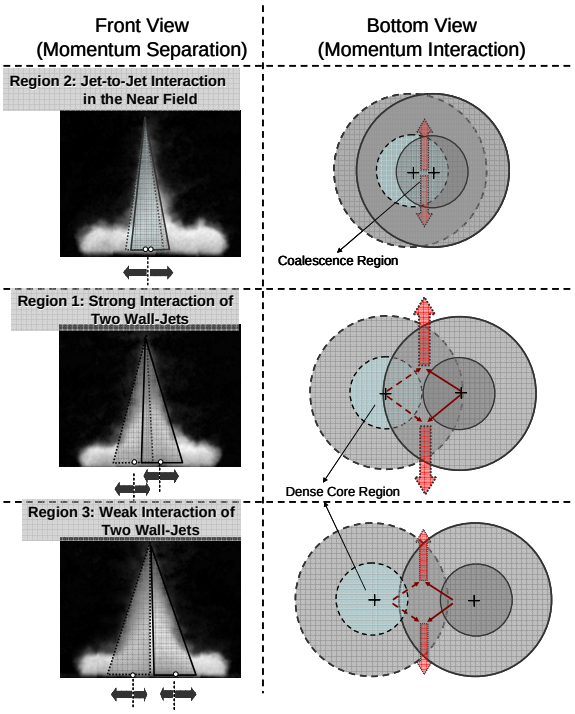

Fig. 7 Mechanism related to the spray tip penetration of group hole nozzle spray

Conclusions

The mechanism related to the spray tip penetration of wall-impinging sprays injected by group-hole nozzles were investigated with the various orifice arrangements. The main findings of this study can be summarized as below.

1. Just after the wall-impingement, the longer spray tip penetration was observed at the vertical view direction and then the spray tip penetration in parallel view direction overtakes the spray tip penetration in vertical view direction due to the momentum interaction between the two impinging jets.
2. The crossing time when the spray tip penetration in parallel view direction starts to overtake that in vertical view direction was delayed as the included angle increased and the injection pressure decreased.
3. The strongest momentum interaction and longest spray tip penetration in parallel view direction were observed around the χ distance of 5.4mm where the strong momentum region of each jet starts to meet just after wall-impingement.
4. The related mechanism on the spray tip penetration was explained based on the momentum separation and momentum interaction of each jet after the wall-impingement.

Acknowledgement – The authors appreciate for the financial support of NEDO and Mazda for this research.

References

1. Nishida, K., Zhang, W. and Manabe, T., *SAE Transaction* 116:421-429 (2008)
2. Su, T. F., Chang, C. T., Reitz, R. D., Farrell, P. V., Pierpont, A. D. and Tow, T. C., 1995, SAE Paper 952360.
3. Siebers, D. and Higgins, B., SAE Paper 2001-01-0530, 2001.
4. Iida, N., Wakimoto, K., Takahashi, S. and Nikolic, D., 2001, SAE Paper 2001-01-1939.
5. Montgomery, D. T., Chan, M., Chang, C. T., Farrell, P. V. and Reitz, R. D., 1996, SAE Paper 962002.
6. Kobori, S., Kamimoto, T. and Kosaka, H., 1996, SAE Paper 960321.
7. Bergstrand, P. and Denbrantt, I., 2001, SAE Paper 2001-01-2010.
8. Hotta, Y., Nakakita, K, Fuyuto, T., Inayoshi, M., Fujiwara, K. and Sakata, I., 2002, SAE Paper 2002-01-1160.
9. Gao, J., Matsumoto, Y. and Nishida, K., *Atomization and Sprays* 19:321-337 (2009)
10. Gao, J., Matsumoto, Y., Nishida, K., 2007, SAE Paper 2007-01-1889.
11. Moon, S., Gao, J., Zhang, Y., Nishida, K. and Matsumoto, Y., 2008, SAE Paper 2008-01-2469.
12. Yamakawa, M., Tadaki, D., Li, T., Zhang, Y. Y. and Nishida, K., 2002, SAE paper 2002-01-1644.
13. Zhang, Y. Y, Yoshizaki, T. and Nishida, K., *Applied Optics* 39:6221-6229 (2000)
14. Desantes, J. M., Arregle, J. and Pator J. V., 1997, SAE Paper 970797.